The Astrophysical Journal Letters, 871:L29 (7pp), 2019 February 1 https://doi.org/10.3847/2041-8213/ab01bd

Whistler Fan Instability Driven by Strahl Electrons in the Solar Wind

I. Y. Vasko[1,2], V. Krasnoselskikh[1,3], Y. Tong[1,4], S. D. Bale[1,4], J. W. Bonnell[1], and F. S. Mozer[1]
[1] Space Sciences Laboratory, University of California, Berkeley, CA 94720, USA
[2] Space Research Institute of Russian Academy of Sciences, Moscow, 177997, Russia
[3] LPC2E/CNRS, Orlean, France
[4] Physics Department, University of California, Berkeley, CA 94720, USA
Received 2019 January 18; revised 2019 January 23; accepted 2019 January 24; published 2019 January 31

Abstract

We present a theoretical analysis of electron heat flux inhibition in the solar wind when a significant portion of the heat flux is carried by strahl electrons. We adopt core-strahl velocity distribution functions typical for the solar wind at 0.3–4 au to demonstrate that strahl electrons are capable of generating highly oblique whistler waves at wave numbers $k\rho_e \sim 1$, where ρ_e is typical thermal electron gyroradius. The whistler waves are driven by electrons in the anomalous cyclotron resonances (the fan instability) and propagate at typical angles of about 70°–80° to the strahl that is usually anti-sunward. The group velocity of the whistler waves is predominantly parallel to the strahl, thereby facilitating efficient scattering of strahl electrons. We suggest that the highly oblique whistler waves drive pitch-angle scattering of strahl electrons, resulting in halo formation and suppressing the heat flux of strahl electrons below a threshold that is shown to depend on β_e. The proposed fan instability is fundamentally different from the whistler heat flux instability driven by the normal cyclotron resonance with halo electrons and being ineffective in suppressing the heat flux of the strahl.

Key words: conduction – instabilities – plasmas – scattering – solar wind – waves

1. Introduction

The electron heat flux in collisionless or weakly collisional plasma can be suppressed below the collisional Spitzer–Härm level (Spitzer & Härm 1953). The heat flux inhibition mechanisms have fundamental applications in the solar wind physics (Hundhausen 1972; Marsch 2006) and astrophysics (Cowie & McKee 1977; Bertschinger & Meiksin 1986; Zakamska & Narayan 2003; Wagh et al. 2014). Spacecraft observations have indicated that wave-particle interactions may inhibit the heat flux in the solar wind (Scime et al. 1994; Gary et al. 1999; Gary & Li 2000), while collisional processes may control the heat flux only at sufficiently low Knudsen numbers (Bale et al. 2013; Landi et al. 2014). In spite of some progress, mechanisms of the heat flux inhibition, particularly in the fast solar wind, are not entirely understood.

In the slow ($\lesssim$400 km s^{-1}) solar wind the electron velocity distribution function (VDF) is often approximated by a dense bi-Maxwellian thermal core and a tenuous suprathermal halo counter-streaming in the plasma frame (Feldman et al. 1975; Maksimovic et al. 1997; Tong et al. 2019). The heat flux is predominantly carried by halo electrons, usually anti-sunward and parallel to magnetic field lines. At sufficiently high heat flux values the so-called "heat flux instability" is capable of generating whistler waves propagating quasi-parallel to the heat flux (Gary et al. 1975, 1994). This instability is driven by halo electrons in the first normal cyclotron resonance; that is, electrons propagating opposite to the whistler waves with a parallel velocity

$$v_{||} = (\omega - \Omega_e)/k_{||}, \quad (1)$$

where ω and $k_{||}$ are the whistler frequency and parallel wave number, Ω_e, is the electron cyclotron frequency. The unstable whistler waves scatter the resonant electrons and may potentially suppress the heat flux (Gary & Feldman 1977), though this process has not been studied in detail. Observations of the heat flux values below a threshold dependent on β_e were interpreted in terms of the heat flux inhibition by whistler waves (Gary et al. 1999; Gary & Li 2000). Simultaneous wave and particle measurements have recently confirmed that the heat flux instability indeed generates quasi-parallel whistler waves in the solar wind (Lacombe et al. 2014; Stansby et al. 2016; Tong et al. 2019), while their role in suppressing the heat flux is still under active investigation.

The major part of the heat flux in the fast ($\gtrsim$500 km s^{-1}) solar wind is carried by strahl electrons, an additional suprathermal field-aligned population usually propagating anti-sunward (Rosenbauer et al. 1977; Pilipp et al. 1987). The heat flux instability driven by counter-streaming core and halo populations (Gary et al. 1975, 1994) can still be excited in the fast solar wind. However, this instability is ineffective in suppressing the heat flux of strahl electrons, because the associated quasi-parallel whistler waves interact efficiently only with electrons satisfying Equation (1); that is, propagating sunward. The mechanism of heat flux suppression in the fast solar wind must be associated with an instability driven by strahl electrons and producing waves scattering strahl electrons. Statistical studies of the electron VDF evolution over radial distances of 0.3–4 au support this point of view (e.g., Štverák et al. 2009; Graham et al. 2017). The decrease of the strahl relative density with increasing radial distance from the Sun and the corresponding increase of the halo relative density indicate formation of the relatively isotropic halo due to the scattering of strahl electrons (Maksimovic et al. 2005; Štverák et al. 2009). The increase of the angular width of the strahl in the velocity space with increasing radial distance from the Sun also indicates the operation of some scattering process (Hammond et al. 1996; Graham et al. 2017).

In this Letter we consider electron VDFs that are typical for the solar wind in order to show that strahl electrons are capable

of generating highly oblique whistler waves at wave numbers $k\rho_e \sim 1$, where ρ_e is a typical electron thermal gyroradius. In contrast to the whistler heat flux instability (Gary et al. 1975, 1994), strahl electrons drive whistler waves via the first anomalous cyclotron resonance

$$v_{||} = (\omega + \Omega_e)/k_{||}. \quad (2)$$

This type of instability is known as the fan instability or the instability of runaway electrons (Kadomtsev & Pogutse 1968; Parail & Pogutse 1978). We underline that the instability is not a beam type (e.g., Sentman et al. 1983), because the contribution of Landau resonant electrons to the growth rate is negative. We argue that highly oblique whistlers generated by the fan instability drive pitch-angle scattering of strahl electrons and suppress their heat flux below a marginal threshold that is shown to depend on β_e.

2. Model VDF and Stability Analysis

We restrict the analysis to a core-strahl electron VDF to focus on the key features of the proposed fan instability and reduce the number of free parameters. The results of the analysis will indicate that the halo population would not be critical for the fan instability. By restricting the analysis to a core-strahl VDF, we also demonstrate the fundamental difference between the fan instability and the whistler heat flux instability driven by halo electrons (Gary et al. 1975, 1994). We adopt the strahl VDF typical for the solar wind at 0.3–4 au (Štverák et al. 2009).

The proton VDF in the plasma rest frame is assumed to be isotropic Maxwellian

$$f_p = \frac{n_0}{(2\pi v_p^2)^{3/2}} \exp\left(-\frac{v^2}{2v_p^2}\right)$$

where n_0 is the plasma density, $v_p = (T_p/m_p)^{1/2}$ is the proton thermal velocity, and T_p is the proton temperature. The core electron VDF is assumed to be isotropic Maxwellian with a bulk flow along the magnetic field lines

$$f_c = \frac{n_c}{(2\pi v_c^2)^{3/2}} \exp\left[-\frac{(v_{||} - \Delta_c)^2}{2v_c^2} - \frac{v_\perp^2}{2v_c^2}\right]$$

where n_c and $v_c = (T_c/m_e)^{1/2}$ are the density and thermal velocity of the core population, and Δ_c is the bulk velocity (usually sunward in the plasma frame). The distribution function of strahl electrons is modeled as follows:

$$f_s = \frac{n_s}{w(2\pi v_s^2)^{3/2}} \frac{2\Theta^{1/2}}{1 + \Theta^{1/2}} \exp\left[-\frac{D(v_{||} - \Delta_s)^2}{2v_s^2} - \frac{v_\perp^2}{2wv_s^2}\right]$$

where n_s and v_s are density and typical thermal spread of the strahl, w controls the angular width of the strahl (or thermal spread anisotropy), Δ_s and

$$D = \begin{cases} 1, & v_{||} > \Delta_s \\ \Theta, & v_{||} < \Delta_s \end{cases}$$

control the skewness of the strahl VDF in the direction along the magnetic field lines. Following Feldman et al. (1975) we impose the zero current condition

$$n_c\Delta_c + n_s\Delta_s + n_s v_s (2/\pi)^{1/2}(1 - \Theta^{-1/2}) = 0.$$

The electron heat flux carried by the core-strahl VDF in the plasma rest frame

$$q_e = 0.5 \int v_{||} m_e v^2 (f_c + f_s) d^3\mathbf{v}$$

is given by a rather cumbersome expression. The heat flux normalized to the typical free-streaming heat flux $q_0 = 1.5 n_0 m_e v_c^3$ depends on five free parameters:

$$n_s/n_0,\ \Delta_s/v_c,\ v_s/v_c,\ w \text{ and } \Theta.$$

When $\Theta \gg 1$ and $w \ll 1$, specific values of Θ and w do not affect heat flux values. In effect, the heat flux depends on n_s/n_0, Δ_s/v_c, and v_s/v_c and lager values of these parameters corresponds to larger heat flux values.

Figure 1 presents the core-strahl VDF at a given set of indicated parameters. Panel (a) shows that the strahl is collimated along the magnetic field. Panel (b) presents the cut of the core-strahl VDF at $v_\perp = 0$ along with a similar cut of the strahl VDF. The strahl VDF is skewed to positive $v_{||}$ due to $\Theta = 20$ and $\Delta_s \geqslant 0$. A slight, almost unnoticeable shift of the core VDF toward negative $v_{||}$ is due to $\Delta_c \neq 0$ required to keep zero current. There are also indicated velocities of electrons in the Landau resonance and the first normal and anomalous cyclotron resonances given by Equations (1) and (2). Panel (c) presents VDF cuts at $v_{||} = 0$. The strahl is unnoticeable in this core-strahl VDF cut, because of the strahl collimation set by $w = 0.1$ and corresponding to the angular width $2v_\perp/v_{||} \sim 2w^{1/2}$ of about 40°, which is typical for the strahl at 1 au (Hammond et al. 1996; Graham et al. 2017).

We perform a stability analysis of whistler waves, assuming that the plasma is weakly unstable; i.e., the growth rate is small with respect to the whistler wave frequency, $\gamma/\omega \ll 1$. The weak instability assumption leads to the standard expression for the growth rate applicable at any wave number and propagation angle (e.g., Mikhailovskii 1974). The linear growth rate is a sum of a damping rate by protons and contributions of electrons in various resonances

$$v_{||} = (\omega + n\Omega_e)/k_{||} \quad (3)$$

where $n = 0$ corresponds to the Landau resonance, $n = 1, 2, \ldots$ to anomalous cyclotron resonances and $n = -1, -2, \ldots$ to normal cyclotron resonances. The growth rate is given by a rather cumbersome analytic expression. At any wave number k ρ_e and wave normal angle θ the growth rate γ/Ω_e depends on seven free parameters

$$\beta_e,\ n_s/n_0,\ \Delta_s/v_c,\ v_s/v_c,\ w,\ \Theta \text{ and } T_p/T_c,$$

where $\rho_e = v_c/\Omega_e$ is typical electron thermal gyroradius, $\beta_e = 8\pi n_0 T_c/B_0^2$ and B_0 is the quasi-static magnetic field. The wave normal angle θ is assumed to be between the wave vector and the strahl propagation direction, the latter of which is either parallel or anti-parallel to the magnetic field.

To shed light on the physics of the proposed fan instability we restrict the range of the free parameters to the most critical ones: β_e, n_s/n_0, and Δ_s/v_c. The proton to electron temperature ratio in the solar wind has a broad statistical distribution, while we use the median value $T_p/T_c = 0.67$ typical at 1 au (e.g., Artemyev et al. 2018; Wilson et al. 2018). For $\Theta \gg 1$ the

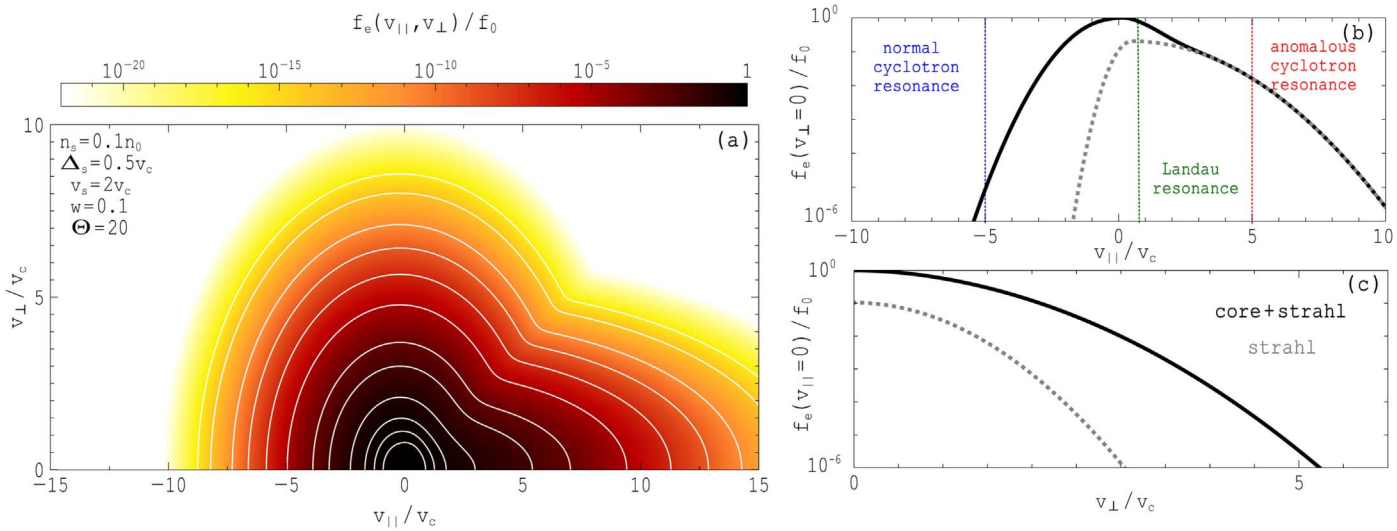

Figure 1. Panel (a) presents the core-strahl electron VDF $f_e(v_{||}, v_\perp)$ normalized to $f_0 = n_0/(2\pi v_c^2)^{3/2}$ for parameters indicated in the panel. Panels (b) and (c) present cuts of the core-strahl and strahl VDFs at $v_\perp = 0$ and $v_{||} = 0$. Panel (b) schematically indicates electrons in the normal cyclotron resonance given by Equation (1), and Landau resonance $v_{||} = \omega/k_{||}$ and anomalous cyclotron resonance given by Equation (2). The proposed fan instability is driven by strahl electrons in the anomalous cyclotron resonance, in contrast to the whistler heat flux instability (Gary et al. 1975, 1994) driven by halo electrons in the normal cyclotron resonance.

specific Θ value does not affect the results of the stability analysis, which is why we choose $\Theta = 20$. We assume the angular width of the strahl to be typical for 1 au, $w = 0.1$, and the thermal spread of the strahl that seems reasonable, $v_s = 2v_c$. Although we present results for fixed T_p/T_c, Θ, w, and v_s/v_c, we performed the stability analysis for other values of these parameters and their major effects are briefly summarized in the next section.

3. Results of the Stability Analysis

Figure 2 presents results of the stability analysis of the core-strahl VDF shown in Figure 1 in a quasi-static magnetic field corresponding to $\beta_e = 1$. Panel (a) shows that whistler waves propagating very oblique to the strahl are unstable at wave numbers $k\rho_e \gtrsim 1$. In physical units the typical growth rate $\gamma/\Omega_e \sim 5 \cdot 10^{-4}$ corresponds to the e-folding time of about a few seconds, which is rather fast instability for the solar wind (here quasi-static field of 5 nT has been used for the estimate). Panel (b) presents the growth rate of whistler waves propagating at a wave normal angle of 78°. The physical nature of the instability is demonstrated by contributions to the growth rate of electrons in various resonances defined by Equation (3). The positive contribution comes from electrons in the anomalous cyclotron resonances with the major input from the first anomalous cyclotron resonance (not shown) due to larger phase space density of these electrons. The contributions of electrons in the Landau and normal cyclotron resonances are negative. The instability is then the so-called "fan instability" (Kadomtsev & Pogutse 1968; Parail & Pogutse 1978). Ions provide a negative contribution, whose absolute value increases with increasing wave number, because at sufficiently large $k\rho_e$ the phase velocity of whistler waves is close to the proton thermal velocity, $\omega/k \sim v_p$. Panel (c) presents the dispersion curve of whistler waves propagating at wave normal angle of 78° and shows that in the plasma rest frame the unstable whistler waves have frequencies $\omega \sim 0.15\ \Omega_e$. The ratio γ/ω is much smaller than one, thereby confirming applicability of the weak instability assumption.

Figure 3 presents results of the stability analysis for core-strahl VDFs at various β_e and n_s/n_0, but at fixed $\Delta_s = 0.5v_c$ as in Figure 2. For $0.01 \leqslant \beta_e \leqslant 5$ and $0.01 \leqslant n_s/n_0 \leqslant 0.2$ we compute the growth rate at various $(k\rho_e, \theta)$ and establish whether or not whistler waves are stable. For unstable whistler waves we identify the wave normal angle $\theta_{\max}$, wave number $k_{\max}$, and frequency $\omega_{\max}$ of the fastest-growing whistler wave. The maximum growth rate $\gamma_{\max}$ in panel (a) shows that at any given β_e the strahl density should be above some threshold for whistler waves to be unstable. The strahl density threshold is well fitted to

$$n_s/n_0 = S_n\,(\beta_e + a_n)^{-\alpha_n}, \tag{4}$$

where $S_n \sim 0.075$, $a_n \sim 0.23$ and $\alpha_n \sim 0.52$. Panels (b) and (c) show that the fastest-growing whistler waves propagate very oblique to the strahl, $\theta_{\max} \sim 70°$–$80°$, at wave numbers $k_{\max}\rho_e \sim 1$–3. Panel (d) shows that in the plasma rest frame the fastest-growing whistler waves have frequencies $\omega_{\max} \sim 0.05 - 0.25\,\Omega_e$. The whistler waves propagate near the resonance cone, $\theta_{\max} \sim \theta_r = \cos^{-1}(\omega_{\max}/\Omega_e) \sim 75°$–$85°$, that is why they have significant electrostatic field along the wave vector (e.g., Helliwell 1965). Because the wave normal angles are comparable to the Gendrin angle, $\theta_g = \cos^{-1}(2\omega_{\max}/\Omega_e) \sim 60°$–$85°$, the group velocity of the whistler waves is almost parallel to magnetic field lines (e.g., Helliwell 1965), thereby facilitating efficient interaction of the whistler waves with the strahl. The phase and group velocities of the considered whistler waves are similar, $\omega/k_{||} \sim \partial\omega/\partial k_{||} \sim \Omega_e d_e \cdot k d_e (1 + k^2 d_e^2)^{-1}$, where d_e is the electron inertial length (e.g., Shklyar et al. 2004). Taking into account that $d_e = \rho_e (2/\beta_e)^{1/2}$, we find that $k_{\max} d_e$ increases from about 0.5 at $\beta_e \sim 5$ to 40 at $\beta_e \sim 0.01$. Therefore, the phase and group velocities of the whistler waves are of the order of the electron thermal velocity, $\omega/k_{||} \sim \partial\omega/\partial k_{||} \sim v_c (k_{\max}\rho_e)^{-1} \sim 0.3\,v_c$.

An analysis similar to that of Figure 3 has been performed for various $0 \leqslant \Delta_s/v_c \leqslant 2$. We have identified the strahl density thresholds and found them to be well fitted to

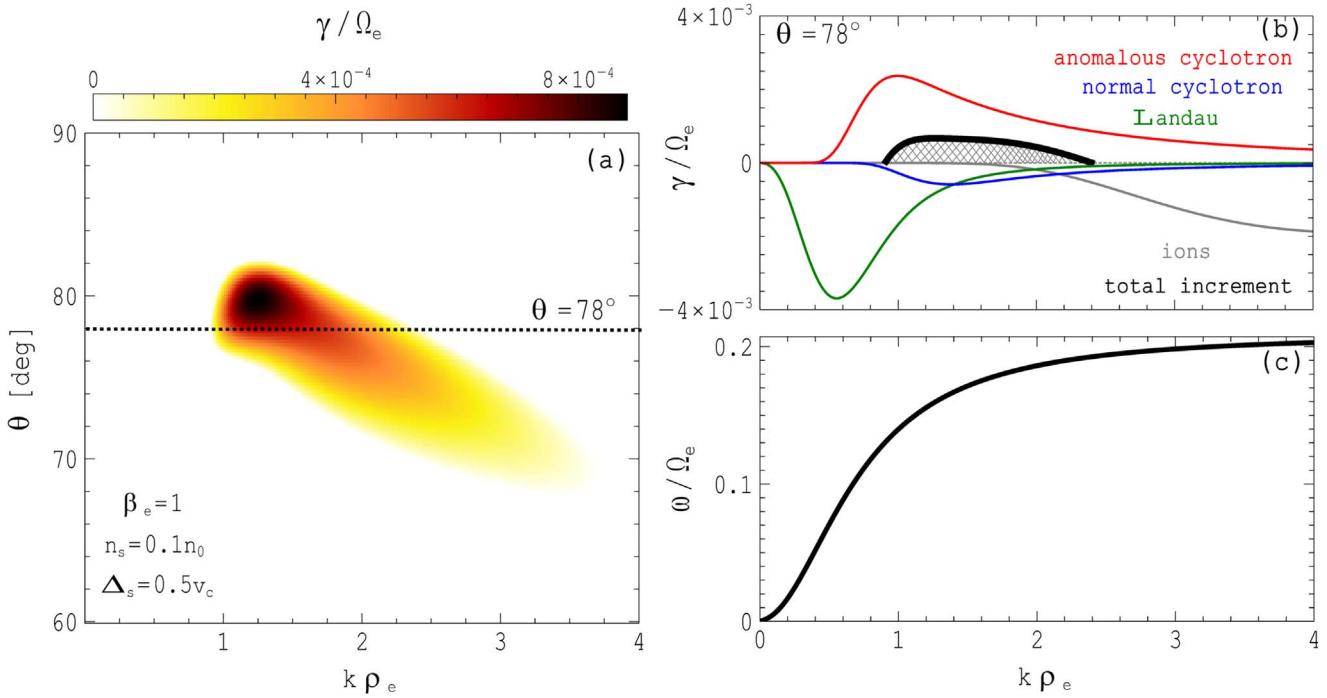

Figure 2. Results of the linear stability analysis of the core+strahl VDF presented in Figure 1 in the magnetic field corresponding to $\beta_e = 1$: (a) the whistler wave growth rate γ normalized to the electron cyclotron frequency Ω_e; only positive growth rates are shown, while negative growth rates are set to zero for visual clarity; (b) the growth rate of whistler waves propagating at wave normal angle $\theta = 78°$ with only positive growth rate shown (black curve and cross-hatched region); there are shown contributions to the total growth rate γ from electrons in all anomalous cyclotron resonances ($n = 1$, 2.... in Equation (3)), normal cyclotron resonances ($n = -1$, -2.... in Equation (3)), and Landau resonance ($n = 0$ in Equation (3)); the damping rate by ions is shown as well (gray curve); (c) the dispersion relation of whistler waves propagating at wave normal angle of $\theta = 78°$.

Equation (4). We note that at $\Delta_s/v_c > 2$ the contribution of the Landau resonant electrons to the growth rate becomes positive at some β_e due to a positive slope in the core-strahl VDF at $v_{||} > 0$. We intentionally restrict our analysis to $\Delta_s/v_c \leqslant 2$, where the contribution of the Landau resonance is negative, to focus on the instability driven by electrons in the anomalous cyclotron resonances and exclude beam-type instabilities driven by electrons in the Landau resonance (see, e.g., Sentman et al. 1983).

Figure 4(a) presents the fitted strahl density thresholds for several $0 \leqslant \Delta_s/v_c \leqslant 2$ with the best-fit parameters given in Table 1. The density threshold n_s/n_0 is generally lower for larger Δ_s/v_c, which is due to a more pronounced skewness of the strahl VDF or, equivalently, larger phase space density of electrons in the anomalous cyclotron resonances. For instance, at $\beta_e \sim 1$ the threshold density is 0.03 for $\Delta_s = 2v_c$ and 0.1 for $\Delta_s = 0$. At some β_e the threshold density can vary non-monotonically with Δ_s/v_c (Figure 4(a)). The reason is that different Δ_s/v_c result in different bulk velocities Δ_c of the core population, thereby affecting the damping rate by electrons in the Landau resonance. Altogether Figure 4(a) clearly shows that at $\beta_e \lesssim a_n \sim 0.1$ the strahl density threshold is independent of β_e, while at $\beta_e \gtrsim a_n$ it depends on β_e as follows $n_s/n_0 \sim S_n \beta_e^{-\alpha_n}$.

Figure 4(b) presents the linear stability thresholds in terms of the normalized electron heat flux q_e/q_0. The heat flux thresholds are obtained by computing q_e/q_0 for the strahl density thresholds in Figure 4(a). The heat flux thresholds are quite well fitted to

$$q_e/q_0 = S_q(\beta_e + a_q)^{-\alpha_q} \quad (5)$$

with the best-fit parameters given in Table 1. At any given β_e the electron heat flux larger than a threshold value makes plasma unstable to the fan instability. For instance, at $\beta_e \sim 1$ the heat flux threshold q_e/q_0 is about 0.2 at $\Delta_s/v_c = 0$ and about 0.4 at $\Delta_s/v_c = 2$. Similarly to the strahl density thresholds, the heat flux threshold is independent of β_e at $\beta_e \lesssim a_q \sim 0.1$, while at $\beta_e \gtrsim a_q$ it depends on β_e as follows $q_e/q_0 \sim S_q \beta_e^{-\alpha_q}$.

We have restricted the stability analysis to the core-strahl VDFs and neglected the halo population. The major effect of the halo population would be the damping of oblique whistler waves by electrons in the Landau resonance. The oblique whistler waves produced by the fan instability have phase velocities of a fraction of the core thermal velocity, $\omega/k_{||} \sim 0.3\, v_c$, that is much smaller than the halo thermal velocity. In the thermal velocity range of the core population the phase space density of core electrons would be much larger than the one of halo electrons. Therefore, the contribution to the damping rate of the oblique whistler waves by Landau resonant core electrons is much larger than the contribution of Landau resonant halo electrons and, hence, the latter can be safely neglected. Finally, we note that in our analysis four free parameters of the core-strahl VDFs have been fixed ($T_p/T_c = 0.67$, $\Theta = 20$, $w = 0.1$ and $v_s = 2v_c$). Below is a short summary of effects of these parameters, while a detailed presentation is left for a separate publication. The increase of T_p/T_c increases the damping rate by protons and, in principle, sufficiently hot protons may quench the instability. For $\Theta \gg 1$ a specific value of this parameter does not affect the stability results. The variation of the angular width w and thermal spread

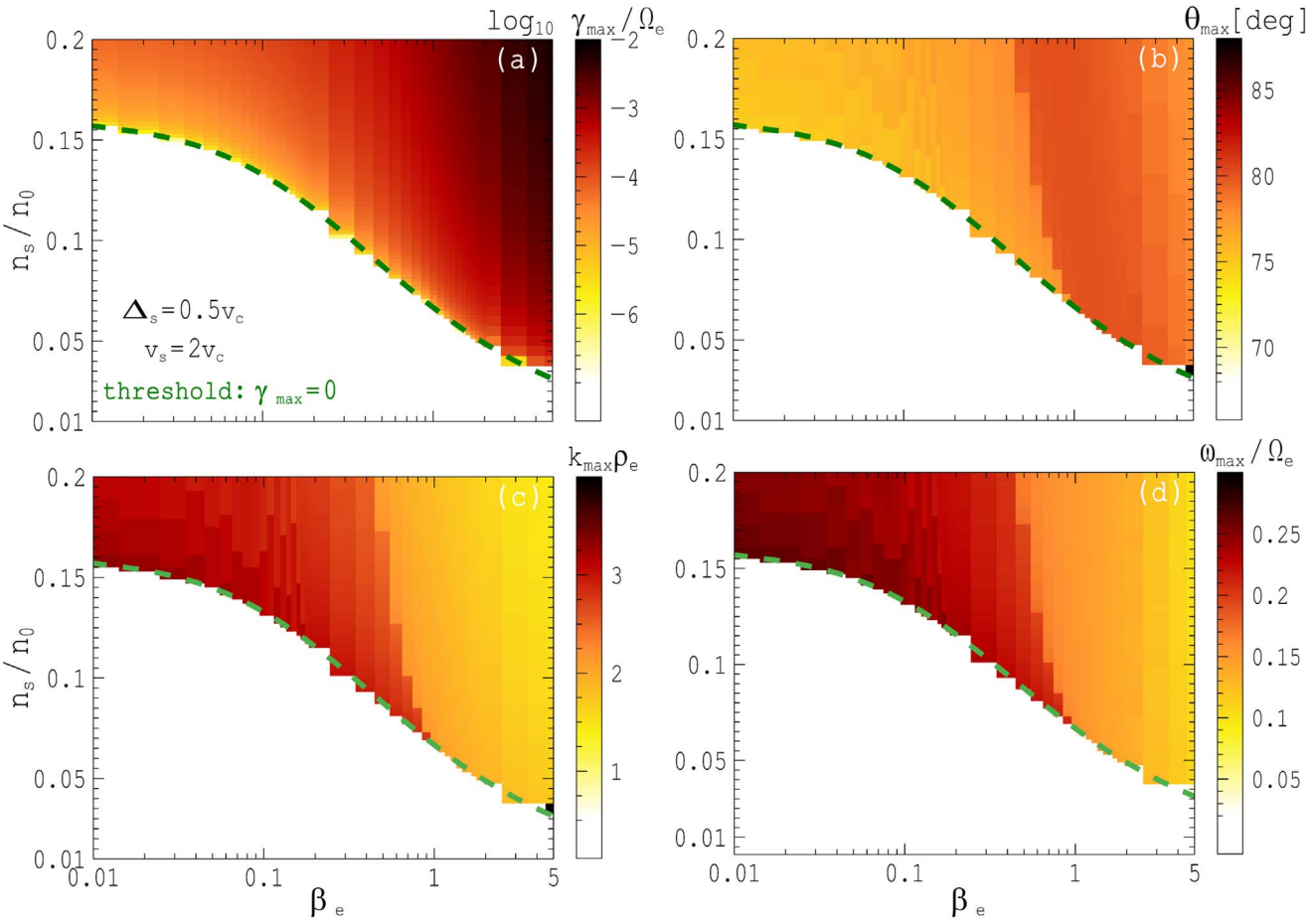

Figure 3. Results of the stability analysis of the core-strahl VDF at various β_e and n_s/n_0 with fixed $\Delta_s = 0.5v_c$ as in Figure 2: (a) the maximum growth rate (white corresponds to stable VDFs); (b, c, d) wave normal angle $\theta_{\max}$, wave number $k_{\max}$ ρ_e, and frequency $\omega_{\max}$ of the fastest-growing whistler wave, where $\rho_e = v_c/\Omega_e$ is the typical electron thermal gyroradius. Panel (a) shows that whistler waves are unstable at sufficiently high strahl densities. The threshold of the strahl density is well fitted to $n_s/n_0 = S_n/(\beta_e + a_n)^{\alpha_n}$ with the best-fit parameters given in Table 1. In all computations we keep $T_p/T_c = 0.67$, $\Theta = 20$, $w = 0.1$ and $v_s = 2v_c$.

v_s/v_c within reasonable ranges does not affect the existence of the fan instability and scaling of the thresholds with β_e.

4. Discussion

We have shown that strahl electrons in the solar wind can generate whistler waves propagating very oblique to the strahl at wave numbers $k\rho_e \gtrsim 1$ or, equivalently, $kd_e \gtrsim (2/\beta_e)^{1/2}$ via the fan instability. This instability has not been found in the recent analysis of Horaites et al. (2018), because the linear stability solver LEOPARD (Astfalk & Jenko 2017) did not allow for the carrying out of the analysis at $kd_e > 1$ and large wave normal angles (P. Astfalk 2019, personal communication). The major effect of the oblique whistler waves on the strahl will be the pitch-angle scattering of strahl electrons in the anomalous cyclotron resonances through the quasi-linear diffusion (Vedenov 1963; Kennel & Petschek 1966) or nonlinear interaction (e.g., Shklyar & Matsumoto 2009; Artemyev et al. 2014). The proposed strahl scattering by the oblique whistler waves generated via the fan instability may potentially resolve several questions in the solar wind physics.

The statistical studies of the electron VDF in the solar wind indicated the operation of some scattering mechanism of the strahl that results in formation of a relatively isotropic halo (Maksimovic et al. 2005; Štverák et al. 2009) and prevents field-aligned focusing of the strahl as it propagates anti-sunward (Hammond et al. 1996; Graham et al. 2017). Vocks et al. (2005) suggested that the strahl is scattered via the first normal cyclotron resonance (1) with quasi-parallel whistler waves propagating sunward, but did not specify mechanisms capable of generating these whistler waves. In fact, it seems uncommon to have sunward propagating quasi-parallel whistler waves in the solar wind. Simultaneous wave and particle measurements in the solar wind have recently shown that quasi-parallel whistler waves are highly likely produced by the whistler heat flux instability and propagate quasi-parallel to the bulk velocity of halo electrons that is usually anti-sunward (Lacombe et al. 2014; Stansby et al. 2016; Tong et al. 2019). Thus, the scattering mechanism of the strahl suggested by Vocks et al. (2005) seems doubtful.

The proposed oblique whistler waves may provide the required scattering of the strahl. The marginal stability threshold given by Equation (4) indicates that at any given β_e the density of the strahl should be below some critical value for the plasma to be stable. Based on the marginal stability threshold we expect the oblique whistler waves to reduce the density of the strahl via the pitch-angle scattering (and formation of a relatively isotropic halo) below some critical value dependent on β_e. The marginal threshold (4) is in qualitative agreement with spacecraft observations indicating that the strahl density decreases with increasing radial distance from the Sun and therefore with increasing β_e (Maksimovic et al. 2005; Štverák et al. 2009). The

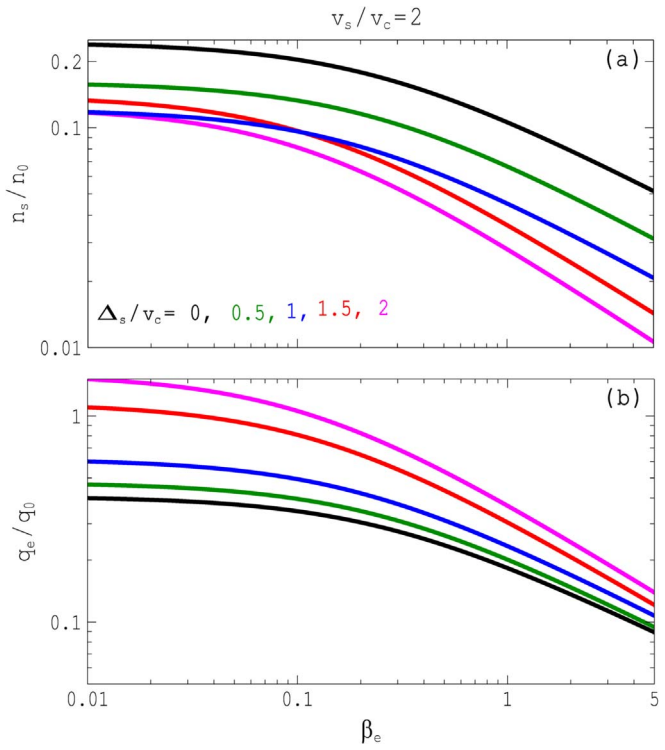

Figure 4. Thresholds on the strahl density $n_s/n_0 = S_n(\beta_e + a_n)^{-\alpha_n}$ and normalized heat flux $q_e/q_0 = S_q(\beta_e + a_q)^{-\alpha_q}$ corresponding to various Δ_s/v_c at $v_s/v_c = 2$. The best-fitting parameters $S_{n,q}$, $a_{n,q}$, and $\alpha_{n,q}$ are given in Table 1. In all computations we keep $T_p/T_c = 0.67$, $\Theta = 20$, $w = 0.1$, and $v_s = 2v_c$.

Table 1
The Best-fit Parameters of the Strahl Density Threshold $n_s/n_0 = S_n(\beta_e + a_n)^{-\alpha_n}$ and Heat Flux Threshold $q_e/q_0 = S_q(\beta_e + a_q)^{-\alpha_q}$ for Various Δ_s/v_c

Δ_s/v_c	S_n/S_q	a_n/a_q	α_n/α_q
0	0.12/0.2	0.23/0.25	0.5/0.5
0.5	0.075/0.22	0.23/0.24	0.52/0.52
1.0	0.05/0.26	0.18/0.19	0.53/0.53
1.5	0.04/0.33	0.12/0.13	0.61/0.6
2.0	0.03/0.39	0.1/0.11	0.63/0.63

detailed analysis of the strahl scattering and halo formation is beyond the scope of this Letter.

We have derived the stability threshold of the fan instability in terms of the normalized electron heat flux q_e/q_0. Interestingly, the stability threshold given by Equation (5) is in general agreement with spacecraft observations (Gary et al. 1999; Tong et al. 2018): at $\beta_e \lesssim 0.1$ the heat flux threshold is only weakly dependent on β_e, while at $\beta_e \gtrsim 0.1$ the heat flux threshold is $q_e/q_0 \sim S\beta_e^{-\alpha}$ with $\alpha \sim 0.5$–0.8. Gary et al. (1994) suggested that quasi-parallel whistler waves produced by the whistler heat flux instability suppress the heat flux in the solar wind, but there is still no consensus on this scenario (Pistinner & Eichler 1998). The whistler heat flux instability is certainly incapable of suppressing the heat flux in the fast solar wind, where the strahl carries the major part of the heat flux. The proposed oblique whistler waves may provide the pitch-angle scattering of the strahl required to suppress the heat flux below the observed thresholds dependent on β_e.

Finally, the potential operation of the fan instability in the solar wind was pointed out previously (Krafft & Volokitin 2010), but there was no analysis that would be applicable for the solar wind conditions. A number of particle-in-cell (PIC) simulations has been recently performed to understand the heat flux inhibition in collisionless plasma in a sustained plasma gradient (Komarov et al. 2018; Roberg-Clark et al. 2018a, 2018b). These simulations have shown that oblique whistler waves at wave normal angles of about 45° and wave numbers $k\rho_e \sim 1$ are produced and suppress the electron heat flux below a threshold dependent on β_e. The simulations support the assumption that oblique whistler waves can suppress the electron heat flux in the solar wind. However, we underline that the PIC simulations are inapplicable for describing the solar wind, because they are initialized with unrealistic electron VDFs and predict unrealistically high whistler wave intensities (whistler wave amplitude comparable to the quasi-static magnetic field) that would have been easily detected in the magnetic field spectra.

5. Conclusion

The linear stability analysis has shown that the strahl in the solar wind can drive very oblique whistler waves propagating at 70°–80° to the strahl at wave numbers $k\rho_e \sim 1$ or, equivalently, $kd_e \gtrsim (2/\beta_e)^{1/2}$. This is the fan instability driven by electrons in the anomalous cyclotron resonances. The stability thresholds for the strahl density and electron heat flux given by Equations (4) and (5) have been derived and tuned out to be in general agreement with previous spacecraft observations. We suggest that the oblique whistler waves provide the scattering of the strahl, thereby resulting in formation of the halo and suppression of the electron heat flux in the solar wind. The group velocity of the unstable whistler waves is in effect parallel to magnetic field lines, thereby facilitating efficient scattering of the strahl. In this Letter the analysis of the fan instability was restricted to $0.01 \leqslant \beta_e \leqslant 5$. The results at low β_e are particularly interesting in the light of the recently launched Parker Solar Probe mission that is going to provide measurements very close to the Sun.

The work of I.Y.V., J.W.B., and F.S.M. was supported by Johns Hopkins University/Applied Physics Lab contract No. 922613 (Radiation Belt Storm Probes-Electric Fields and Waves). V.K. acknowledges the financial support through the grant of CNES (Parker Solar Probe). Y.T. and S.D.B. were supported in part by NASA contract NNN06AA01C. I.V. and V.K. thank A. Artemyev and I. Kuzichev for discussions.

ORCID iDs

I. Y. Vasko https://orcid.org/0000-0002-4974-4786
V. Krasnoselskikh https://orcid.org/0000-0002-6809-6219
Y. Tong https://orcid.org/0000-0002-3354-486X
S. D. Bale https://orcid.org/0000-0002-1989-3596

References

Artemyev, A. V., Angelopoulos, V., & McTiernan, J. M. 2018, JGRA, 123, 9955
Artemyev, A. V., Vasiliev, A. A., Mourenas, D., Agapitov, O. V., & Krasnoselskikh, V. V. 2014, PhPl, 21, 102903
Astfalk, P., & Jenko, F. 2017, JGRA, 122, 89
Bale, S. D., Pulupa, M., Salem, C., Chen, C. H. K., & Quataert, E. 2013, ApJL, 769, L22

Bertschinger, E., & Meiksin, A. 1986, ApJL, 306, L1
Cowie, L. L., & McKee, C. F. 1977, ApJ, 211, 135
Dennel, C. F., & Petschek, H. E. 1966, JGR, 71, 1
Feldman, W. C., Asbridge, J. R., Bame, S. J., Montgomery, M. D., & Gary, S. P. 1975, JGR, 80, 4181
Gary, S. P., & Feldman, W. C. 1977, JGR, 82, 1087
Gary, S. P., Feldman, W. C., Forslund, D. W., & Montgomery, M. D. 1975, JGR, 80, 4197
Gary, S. P., & Li, H. 2000, ApJ, 529, 1131
Gary, S. P., Scime, E. E., Phillips, J. L., & Feldman, W. C. 1994, JGR, 99, 23391
Gary, S. P., Skoug, R. M., & Daughton, W. 1999, PhPl, 6, 2607
Graham, G. A., Rae, I. J., Owen, C. J., et al. 2017, JGRA, 122, 3858
Hammond, C. M., Feldman, W. C., McComas, D. J., Phillips, J. L., & Forsyth, R. J. 1996, A&A, 316, 350
Helliwell, R. A. 1965, Whistlers and Related Ionospheric Phenomena (Stanford, CA: Stanford Univ. Press)
Horaites, K., Astfalk, P., Boldyrev, S., & Jenko, F. 2018, MNRAS, 480, 1499
Hundhausen, A. J. 1972, Coronal Expansion and Solar Wind, XII, Vol. 5 (Berlin: Springer)
Kadomtsev, B. B., & Pogutse, O. P. 1968, JETP, 26, 1146
Komarov, S., Schekochihin, A. A., Churazov, E., & Spitkovsky, A. 2018, JPlPh, 84, 905840305
Krafft, C., & Volokitin, A. 2010, PhPl, 17, 102303
Lacombe, C., Alexandrova, O., Matteini, L., et al. 2014, ApJ, 796, 5
Landi, S., Matteini, L., & Pantellini, F. 2014, ApJL, 790, L12
Maksimovic, M., Pierrard, V., & Riley, P. 1997, GeoRL, 24, 1151
Maksimovic, M., Zouganelis, I., Chaufray, J.-Y., et al. 2005, JGRA, 110, A09104
Marsch, E. 2006, LRSP, 3, 1
Mikhailovskii, A. B. 1974, Theory of Plasma Instabilities, Instabilities of a Homogeneous Plasma, Vol. 1 (Berlin: Springer)
Parail, V. V., & Pogutse, O. P. 1978, NucFu, 18, 303
Pilipp, W. G., Miggenrieder, H., Montgomery, M. D., Mühlhäuser, K.-H., Rosenbauer, H., & Schwenn, R. 1987, JGR, 92, 1075
Pistinner, S. L., & Eichler, D. 1998, MNRAS, 301, 49
Roberg-Clark, G. T., Drake, J. F., Reynolds, C. S., & Swisdak, M. 2018a, PhRvL, 120, 035101
Roberg-Clark, G. T., Drake, J. F., Swisdak, M., & Reynolds, C. S. 2018b, ApJ, 867, 154
Rosenbauer, H., Schwenn, R., Marsch, E., et al. 1977, JGZG, 42, 561
Scime, E. E., Bame, S. J., Feldman, W. C., et al. 1994, JGR, 99, 23401
Sentman, D. D., Thomsen, M. F., Gary, S. P., Feldman, W. C., & Hoppe, M. M. 1983, JGR, 88, 2048
Shklyar, D., Chum, J., & Jirícek, F. 2004, AnGeo, 22, 3589
Shklyar, D., & Matsumoto, H. 2009, SGeo, 30, 55
Spitzer, L., & Härm, R. 1953, PhRv, 89, 977
Stansby, D., Horbury, T. S., Chen, C. H. K., & Matteini, L. 2016, ApJL, 829, L16
Štverák, Š., Maksimovic, M., Trávníček, P. M., et al. 2009, JGRA, 114, A05104
Tong, Y., Bale, S. D., Salem, C., & Pulupa, M. 2018, arXiv:1801.07694
Tong, Y., Vasko, I. Y., Pulupa, M., et al. 2019, ApJL, 870, L6
Vedenov, A. A. 1963, JNuE, 5, 169
Vocks, C., Salem, C., Lin, R. P., & Mann, G. 2005, ApJ, 627, 540
Wagh, B., Sharma, P., & McCourt, M. 2014, MNRAS, 439, 2822
Wilson, L. B., III, Stevens, M. L., Kasper, J. C., et al. 2018, ApJS, 236, 41
Zakamska, N. L., & Narayan, R. 2003, ApJ, 582, 162